Self-organization of Spinal Reflexes Involving Homonymous, Antagonist and Synergistic Interactions

Hugo Gravato Marques[1,2], Kristin Völk[1], Stefan König[1], and Fumiya Iida[1]

[1] ETH,
Dep. of Mechanical and Process Engineering, BIRL,
Zurich 8092, Switzerland
hgmarques@gmail.com
[2] University of Zurich,
Institute for Informatics, AI Lab.,
Zurich 8050, Switzerland

Abstract. Recent results in spinal research are challenging the historical view that the spinal reflexes are mostly hardwired and fixed behaviours. In previous work we have shown that three of the simplest spinal reflexes could be self-organised in an agonist-antagonist pair of muscles. The simplicity of these reflexes is given from the fact that they entail at most one interneuron mediating the connectivity between afferent inputs and efferent outputs. These reflexes are: the Myotatic, the Reciprocal Inibition and the Reverse Myotatic reflexes. In this paper we apply our framework to a simulated 2D leg model actuated by six muscles (mono- and bi-articular). Our results show that the framework is successful in learning most of the spinal reflex circuitry as well as the corresponding behaviour in the more complicated muscle arrangement.

1 Introduction

Historically the spinal cord has been viewed as a rather inflexible system, composed of hardwired reflexes that have very limited degrees of adaptability and plasticity [9][1]. However, recent studies have shown that at least some of these circuits can be adapted by changing the contingent (i.e. temporally correlated) sensor and motor information. In Petersson et al. [7] showed that the delivery of false tactile feedback in response to spontaneous muscle twitches (SMTs) can systematically modify the response of the spinal withdrawal reflex. One of the major contributions of this work was the identification of SMTs as a major driving force in the adaptive process. SMTs consist of involuntary contractions that can activate muscles independently [1][2]. This kind of motor activity can be

[1] This research was funded by the Swiss SNF, Grant No. PP00P2123387/1, the Swiss NCCR Robotics, and the EU's FP7, Cognitive Systems, Interaction, Robotics no. 207212 – eSMCs.

[2] Note that SMTs are not the only mechanism of spontaneous motor activity (see [1]).

T. Ziemke, C. Balkenius, and J. Hallam (Eds.): SAB 2012, LNAI 7426, pp. 269–278, 2012.

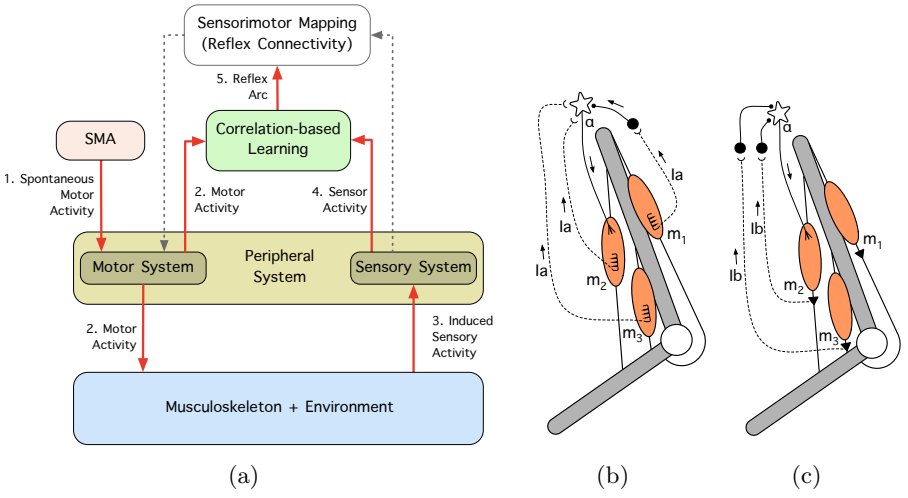

Fig. 1. (a) The framweork proposed; it works as follows: (1) spontaneous motor activity (SMA) produces contractions of individual muscles (SMTs), (2) the muscle contractions produce forces which are propagated through the musculoskeletal system (as well as throughout the environment where it is embedded), (3) the changes produced in the musculoskeletal system are captured by the different sensors, which (4) convert them into sensor activity, (5) the correlation between the sensor and motor activity is used to learn the reflex circuitry between each sensor and motor pair. (b-c) The spinal circuitry of the three reflexes investigated: b) the Myotatic reflex and the Reciprocal Inhibition reflex (which are supposed to counteract the effects of external loads), and c) the Reverse Myotatic reflex (which is supposed to prevent muscles from producing too high forces). The stars represent α-motoneurons, the large solid circles represent inhibitory interneurons, semi-circled arcs represent excitatory connections, small solid circles represent inhibitory connections, the dashed lines represent afferent inputs from a) Ia fibers and b) Ib fibers, m_i indicates an abstract muscle i, and the arrows represent the flow of information. The spirals in (b) represent the muscle spindles, the filled triangles in (c) represent the Golgi-tendon organs. The reflex circuitry has been abstracted from [8, pp.79-86,209-15, 256-60]

observed during active sleep from fetuses to adults, and it has been argued to contribute strongly to the development of the human motor system.

In previous work we proposed a framework to self-organize spinal reflexes from the contingent sensor and motor information induced during SMTs (see Fig.1a). These reflexes were: the Myotatic, the Reciprocal Inhibition and the Revere Myotatic reflexes (see Fig. 1b-c). These reflexes consist of very small local circuits (they include at most one interneuron in their reflex arcs) that coordinate muscle information. They are carried out through two types of afferent inputs: the Ia and the Ib fibers. The Ia fibers estimate changes in the muscle length as well as (positional) muscle length [4], and the Ib fibers respond to small variations in muscle force [5].

In the human spine the circuitry of these reflexes involve mainly three types of sensorimotor (muscle) interactions: homonymous (i.e. interactions between the same muscle), antagonistic (i.e. interaction between muscles that move a joint in opposing directions), and synergistic (i.e. interaction between muscles that move a joint in the same direction). In our previous work we have successfully self-organized the three reflexes in a minimalistic setup involving homonymous and antagonist interactions using a pair of simulated mono-articular muscles [6]. In this paper, our goal is to test the framework in a more complicated muscle arrangement which comprises six muscles and includes synergistic interactions provided by bi-articular muscles.

The remainder of this paper is organized as follows. The second section describes the implementation of our framework (here we will only provide the details relevant to understand this paper; more information can be found in [6]). The third section provides the results obtained. The fourth section discusses the results. And the fifth section concludes the paper and gives some directions for future work.

2 Methods: Implementation of Framework Models

Our framework consists of five interacting models: a musculoskeletal model (and its environment), a peripheral model, a model of spontaneous motor activity (SMA), a learning model based on the correlations between sensor and motor activity, and a model of the reflex sensorimotor mapping (see Fig.1). The first four models are involved in the learning of the reflexes (learning stage) and the last model is responsible for triggering the reflex activity (testing stage). The interaction between these models is described in Fig. 1. In this section we will describe the implementation of each of these models.

reflex learning from

2.1 Implementation of the Musculoskeletal System and the Environment

Our musculoskeletal system consists of a 2D virtual model of a leg actuated by six muscles (see Fig. 2a). We have called these muscles: Glutei (G), Iliacus (I), Rectus Femuris (RF), Long Biceps (LB), Short Biceps (SB), and Vast Group (VG), which in the human leg produce approximately the same type of (flexion and extension) motions. The muscles LB and RF are bi-articular muscles (represented as dashed lines in Fig. 2a). The simulation of the leg dynamics is carried out in SimMechanics/Simulink. The skeleton model consists of three rigid bodies: the pelvis, the femur and the tibia, which are connected by hinge joints (hip and knee). In our simulation the pelvis is fixed in space, and only the femur ($mass = 1kg$, $length = 0.5m$) and tibia ($mass = 0.5kg$, $length = 0.5m$) are allowed to move (e.g. due to gravity).

Each muscle is simulated as a straight line between two rigid bodies (see Fig. 2b). The muscle model used in our investigation is based on a 2-element non-linear Hill model [3] [10]. The two elements in the model are an active contractile

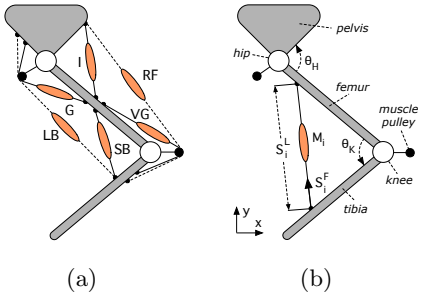

Fig. 2. Diagram of the leg model implemented. a) the geometric arrangement of the six muscles in the leg: the Glutei (G), the Iliacus (I), the Rectus Femuris (RF), the Long Biceps (LB), the Short Biceps (SB), and the Vast Group (VG); bi-articular muscles are shown in dashed lines; b) an abstraction of the muscle model used, M_i corresponds to the motor activity of α-motoneurons of muscle i. The filled circles represent pulleys which simulate the way muscles wrap around the joints. Each muscle has two sensors, S_i^L and S_i^F, which are used to estimate the length and force (respectively) of muscle i.

element in parallel with a passive elastic element. The contractile element models the active force generated by the muscle fibers. This element includes a damping mechanism that simulates the force-velocity relation of biological muscles. The passive elastic element models the muscle fiber's resistance to deflection.

The force produced by muscle i at its attachment points is given by:

$$F_{M_i} = F_{CH_i} + F_{SH_i}, \qquad F_{CH_i} = \frac{M_i}{1 + C \cdot \dot{l}_i}, \qquad F_{SH_i} = K \cdot \Delta l_i \tag{1}$$

where F_{CH_i} is the force produced by the Hill contractile element of muscle i and F_{SH_i} is the force produced by the passive spring element of muscle i, C is a constant damping factor, K is a constant spring factor, M_i is the motor activation of motor i, $\dot{l}_i$ is the rate of change of the muscle length relative to muscle i, Δl_i is the passive deformation of muscle i. In biology the force generated by the passive spring element of the muscle, F_{SH_i}, is significantly smaller than the force generated by the contractile element, F_{CH_i}. To achieve these properties we set $K = 10$ and $C = 0.5$. At the beginning of both the learning and testing stages, the model starts with all muscles relaxed ($M = 0$). In this condition the leg falls straight down due to the effect of gravity.

2.2 Implementation of Peripheral System

The peripheral system includes motor and sensing elements. The sensor elements consist of analogues to α-motoneurons the activity of which determines the muscle contraction, M_i. On the sensing side we simulate two types of sensors (see Fig. 2b): one that measures the length of the muscle, S_i^L (i.e. the distance between the two attachment points), and one that measures the force at the attachment points, S_i^F; when referring to sensors indiscriminately we will simply

use the symbol S. In our simulation the sensor activity consists of the derivatives of these sensor inputs ($\dot{S}_i^L$ and $\dot{S}_i^F$), which provide qualitative analogues of the Ia and Ib afferent fibers.

2.3 Implementation of Correlation-Based Learning

This process identifies the reflex circuitry based on the correlation between sensor and motor activity. All possible pairs of sensor and motor elements are considered. We use the method of motor-directed somatosensory imprinting (MDSI), which has been used to explain the self-organization of the withdrawal reflex [7]. This method uses the anti-Hebbian rule [2] which is given by the additive inverse of the temporal correlation between the sensor and motor activity. It is important to mention here that despite the fact that the anti-Hebbian rule has been used to justify plastic phenomena in the spinal cord [7], such a rule (to our knowledge) has not yet been explicitly identified. The reflex connectivity, Q, is then given by:

$$Q_{i,j} = -\eta_{ij} \sum_{t=1}^{T} M_{i,t} \cdot \dot{S}_{j,t}, \qquad \eta_{ij} = \left[max(\dot{S}_j) \sum_{t=1}^{T} M_{i,t} \right]^{-1} \tag{2}$$

where η_{ij} is a normalization factor, $M_{i,t}$ is the motor activity of motor i at timestep t, $\dot{S}_{i,t}$ is the sensor activity of sensor j at timestep t, and T is the number of timesteps taken by the learning process. Excitatory connections are characterized by positive values and inhibitory connections by negative values. The strength of each connection is given the magnitude, $|Q|$.

2.4 Implementation of Spontaneous Motor Activity

During the learning stage the generation of single muscle twitches is done by sequentially contracting one muscle after the other, generating a total of six SMTs. Each twitch consists of a short rectangular pulse of amplitude $1mu$ (motor units) and duration of $1s$. The time between twitches is set to a value large enough to allow the system to stop oscillating.

2.5 Implementation of Sensorimotor Mapping

The testing of the reflex behaviours is carried out exclusively by the sensorimotor mapping model. The testing consists of applying an external force, D at the bottom of the tibia ($D = 1N$ applied in the x direction). This causes both the femur and the tibia to rotate counterclockwise (see Fig. 2b), which causes the length of the muscles G, LB and SB to increase and the length of the muscles I, RF and VG to decrease. The reflex behavior, M_i, is then triggered by the measured sensor stimulation at each sensor S_j weighted by the respective connection $Q_{i,j}$:

$$M_{i,t} = G \cdot \sum_{j=1}^{m} A_{i,j,t}, \qquad A_{i,j,t} = Q_{i,j} \frac{\dot{S}_{j,t}}{max(\dot{S}_{j,t})} \tag{3}$$

where G is a dimensionless value with the reflex gain, m is the number of motors in the system, t is time, and $A_{i,j}$ is the output of the inhibitory or excitatory connection. In biology the positive or negative effect of a connection on a given neuron is defined by the nature of the connection (excitatory and inhibitory respectively); negative connections can only decrease the activity of afferent neurons, and excitatory connections can only increase the activity of afferent neurons. To ensure these effects in our simulation, we add a condition where we define that inhibitory connections (i,e. those where $Q_{i,j} < 0$) can only have a negative impact on the motor activity; and that excitatory connections (i,e. those where $Q_{i,j} > 0$) can only have a positive impact on the motor activity. This is achieved by setting $A_{i,j} = 0$ whenever $\dot{S}_{j,t} < 0$.

3 Results

Figure 3 shows the sensory activity induced in response to SMTs in different muscles. The muscles shown include the three types of muscle interactions investigated here (i.e. homonymous, antagonistic and synergistic). Figure 3a-c illustrates the reaction of the length sensors to the contraction of one muscle induced by a SMT in this muscle. Figure 3d-e shows the reaction of the force sensors to the same SMTs. As can be seen, all the SMTs induce causal information in all the length sensors of each muscle, whereas the force sensors are affected only by contractions of the homonymous muscle. This is because when a muscle is relaxed the only force in the muscle is due to the passive spring element which has a negligible magnitude when compared with the active force that can be produced by the contractile element of the muscle.

The data shown in Fig. 3 suggest causal relations between force sensors and homonymous muscles, and between length sensors and homonymous, antagonistic and synergistic muscles. The learned connectivity matrix, Q, is shown in Fig. 4a. In relation to the force sensors we obtain inhibitory connections with the homonymous muscles only (e.g. between $\dot{S}^F_G$ and M_G); all the other connections obtained have negligible magnitudes (≤ 0.001). This connectivity corresponds to that of the Reverse Myotatic reflex for homonymous muscles. In comparison to the analogue biological circuitry (see Fig. 1c) we fail to obtain inhibitory connections between force sensors and synergistic muscles (see Sect. 4 for discussion).

In relation to the length sensors we obtain excitatory connections with homonymous muscles (e.g. between $\dot{S}^L_G$ and M_G) as well as with synergistic muscles (e.g. between $\dot{S}^L_{LB}$ and M_G). This connectivity pattern is in line with the connectivity of the Myotatic as shown in Fig. 1b. The only exception to this rule is observed between $\dot{S}^L_{VG}$ and M_{RF} where we obtain an inhibitory connection. This connection is caused by the fact that the twitches are performed with the leg hanging down in a straight line due to gravity. In this position the contraction of the RF muscle leads to a flexion of the hip, which causes the Tibia to swing slightly backwards due to gravity; this in turn causes a knee flexion instead of the knee extension that would typically be observed when the RF contracts.

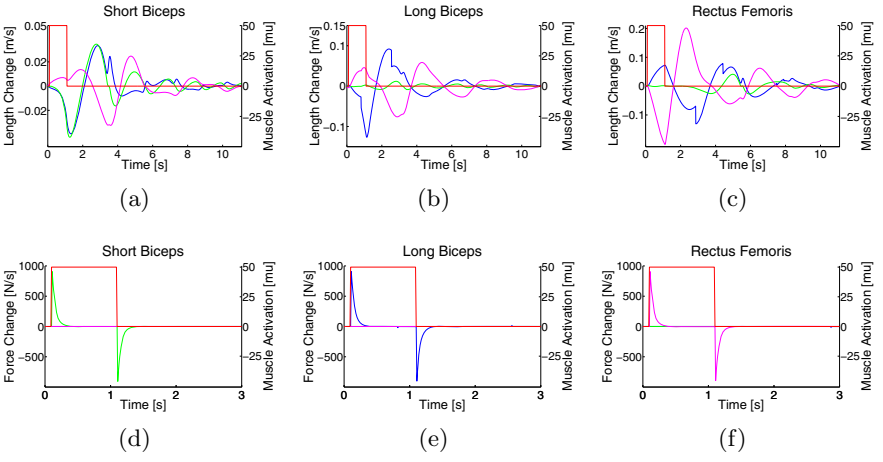

Fig. 3. (a)-(c): The changes in muscle length of the Short Biceps (green), the Long Biceps (blue) and the Rectus Femoris (magenta) in response to a SMT (red) carried out by a) the Short Biceps, b) the Long Biceps and c) the Rectus Femoris. (d)-(f): The changes in muscle force of the Short Biceps (green), the Long Biceps (blue) and the Rectus Femoris (magenta) in response to a SMT (red) carried out by d) the Short Biceps, e) the Long Biceps and f) the Rectus Femoris.

In addition we obtain inhibitory connections between the length sensors and antagonist muscles (e.g. between $\dot{S}^L_{RF}$ and M_G), which is consistent with the connectivity observed in relation to the Reciprocal Inhibition reflex (see Fig. 1b). Figure 4b provides a more clear representation of the connectivity of the length sensors with the homonymous, antagonist and synergistic muscles.

Connections can also be found between muscles in distal joints, (e.g. the excitatory connection between $\dot{S}^L_I$ and M_{SB}). This connectivity is present because a movement produced at a given joint can induce movement in other joints (e.g. due to gravity or inertia). Connections between muscles at distal joints are also present in the human spinal cord but they will not be analysed here. Connections between length sensors and motor elements not shown in the Q-matrix of Fig. 4a have very small magnitudes (≤ 0.006) and do not have any behavioral relevance.

The resulting reflex behavior is shown in Fig. 5. The figure shows the response of the six muscles to the external perturbation (see Sect. 2.5), in three different conditions: using no reflexes ($G = 0$), using the non-modulated Q matrix ($G = 1$) and using a modulation gain of $G = 3$. By comparing the angles of the knee and hip joint at reflex application to those without reflexes, it can be seen that the action of the reflexes has the effect of dampening the system, similar to the function of a proportional controller. Higher gains cause a higher dampening of the system and result in an increase of the overall motor activity. Additionally the muscle activations for agonist-antagonist pairs tend to be opposite (e.g. between RF and LB, or between G and I). Synergistic muscles on the other hand tend to be recruited at the same time (e.g. LB and SB, or RF and I).

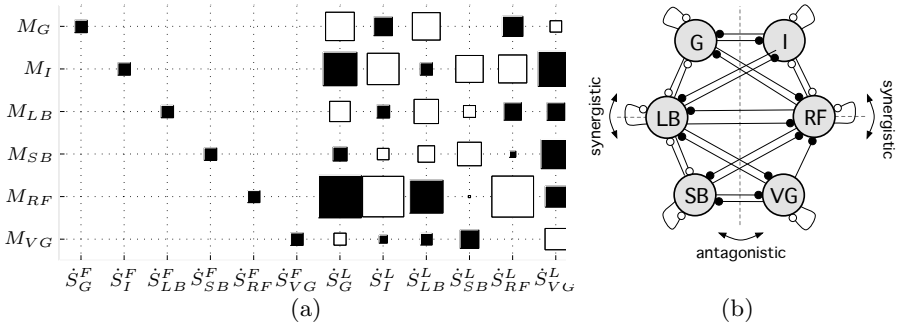

Fig. 4. The reflex circuitry obtained using our framework a) in a matrix and b) in a graph representations. Filled squares and circles represent inhibitory connections and empty squares and circles represent excitatory connections. In a) the strength of each connection is given by the square size; all the sizes have been normalized by the weight of the highest connection. In b) are shown only the interactions of length sensors with homonymous, antagonist and synergistic muscles.

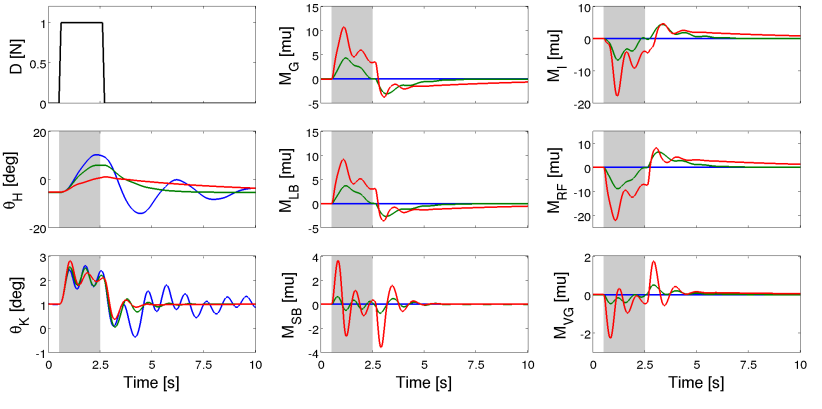

Fig. 5. Muscle-related activity generated by the reflex circuitry in reaction to an external disturbance of $1N$ in the x-direction imposed on the endpoint of the Tibia. Left side from top to bottom: 1) the external disturbance, 2) angle of the hip joint, and 3) angle of the knee joint. In the middle from top to bottom, activations of: 1) Glutei , 2) Long Biceps, and 3) Short Biceps (mu stands for motor units). Right side from top to bottom, activations of: 1) 1) Iliacus, 2) Rectus Femoris, 3) Vast Group. Each line in the figure shows three experimental conditions: blue, no reflex activity, $G = 0$; green, non-modulated reflex activity $G = 1$, and red, modulated reflex activity $G = 5$.

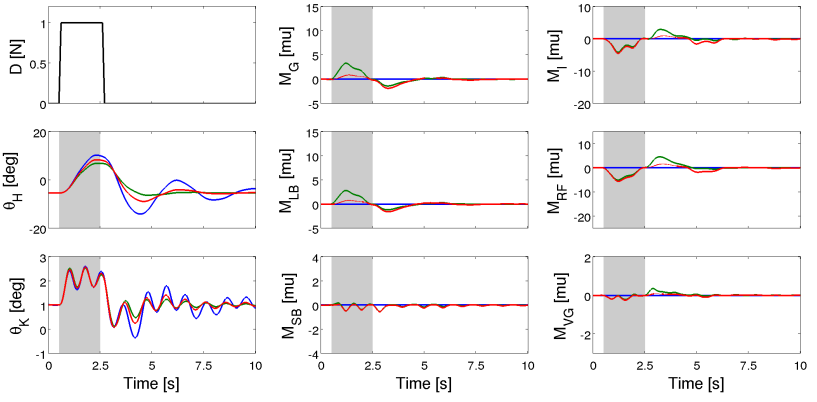

Fig. 6. The Reverse Myotatic reflex. Same elements as Fig. 5, but the three conditions shown are: blue, no reflex activity, $G = 0$; green, non-modulated reflex activity $G = 1$, and red, *dual-gain* condition (see text).

The muscle activity produced by the Myotatic and the Reciprocal Inhibition reflexes is shown in Fig. 5. In relation to the Myotatic reflex it can be observed that the increase in the length of the muscles G, LB and SB (imposed by the external perturbation) results in an increase of motor activity in these muscles[3]. In relation to the Reciprocal Inhibition reflex it can be observed that the decrease in the length of the muscles I, RF and VG (imposed by the external perturbation) results in a decrease of motor activity in these muscles (see also footnote).

The activity of the Reciprocal Inhibition reflex is slightly more complicated to visualize since in the range of forces we use the force component contributes very little to the overall muscle activity. To give expression to the force component we set a higher gain ($G_F = 50$) to the force elements in the matrix Q, while keeping the gains of the length elements ($G_L = 1$); we call this condition *dual-gain*. In this condition the effects of the Myotatic reflex alternate constantly with those of the Reverse Myotatic reflex, leading to peaks that alternate between positive and negative muscle activity. To show the overall muscle activity in this condition we filter all the muscle responses (in the three conditions) with a Savitzky-Golay filter of order 3 and window size of 51 (*sgolayfilt* function in Matlab). Fig. 6 shows the muscle activity in the *dual-gain* condition in comparison with that in $G = 0$ (no reflex activity) and $G = 1$ (non-modulated reflex activity). As can be seen in the *dual-gain* condition the Myotatic reflex leads to a generalized decrease of muscle activity in all the active muscles ($M_i > 0$). This is due to the inhibitory nature of the Reverse Myotatic reflex circuitry. In addition, it can be

[3] The length increase of the SB muscle, as well as the length decrease of the VG muscle, can only be observed immediately after the disturbance is applied; the small oscillations that are observed afterwards are due to the impact of gravity in the vertical alignment of the leg mentioned above.

seen from the joint angles that the system gets less damped than in the $G = 1$ condition, which is due to the overall decrease of muscle activity.

4 Discussion and Conclusions

Our results show that most of the circuitry and the behavior obtained are consistent with human data. Relative to the Myotatic reflex we obtain, excitatory connections between length sensors and motor elements of homonymous and synergistic muscles. Relative to the Reciprocal Inhibition reflex we obtain inhibitory connections between length sensors and motor elements of antagonist muscles. And relative to the Reverse Myotatic reflex we obtain inhibitory connections between the force sensors and motor elements of the homonymous muscles. The only circuits that are systematically absent in our results (and are present in humans) are those involving connections between force sensors of a muscle and motor elements of the synergistic muscles (see Fig.1b-c).

In reality the contraction of one muscle should not induce force information on any other muscle. Our hypothesis is that the connectivity between force sensors and motor elements of synergistic muscles is accidental; it is formed because synergistic muscles are often recruited at the same time, which prevents casual sensorimotor relations from being fully disambiguated. We are currently working ways of exploiting synchronous muscle activations during SMA.

References

1. Blumberg, M.S., Lucas, D.E.: Dual mechanisms of twitching during sleep in neonatal rats. Behav. Neurosci. 108, 1196–1202 (1994)
2. Földiák, P.: Forming sparse representations by local anti-hebbian learning. Biol. Cybern. 64, 165–170 (1990)
3. Hill, A.V.: The heat of shortening and dynamics constants of muscles. Proc. R. Soc. Lond. B 126(843), 136–195 (1938)
4. Hulliger, M.: The mammalian muscle spindle and its central control. Rev. Physiol. Bioch. P. 101, 1–110 (1984)
5. Jami, L.: Golgi tendon organs in mammalian skeletal muscle: Functional properties and central actions. Physiol. Rev. 72(3), 632–666 (1992)
6. Marques, H.G., Imtiaz, F., Iida, F., Pfeifer, R.: Self-organisation of reflexive behaviour from spontaneous motor activity (2012) (under review)
7. Petersson, P., Waldenström, A., Fåhraeus, C., Schouenborg, J.: Spontaneous muscle twitches during sleep guide spinal self-organization. Nature 424, 72–75 (2003)
8. Pierrot-Deseilligny, E., Burke, D.: The Circuitry of the Human Spinal Cord. Cambridge University Press (2005)
9. Schouenborg, J.: Somatosensory imprinting in spinal reflex modules. Journal of Rehabilitation Medicine (41 suppl.), 73–80 (2003)
10. Zajac, F.E.: Muscle and tendon: properties, models, scaling and application to biomechanics and motor control. Crit. Rev. Biomed. Eng. 17(4), 359–410 (1989)